

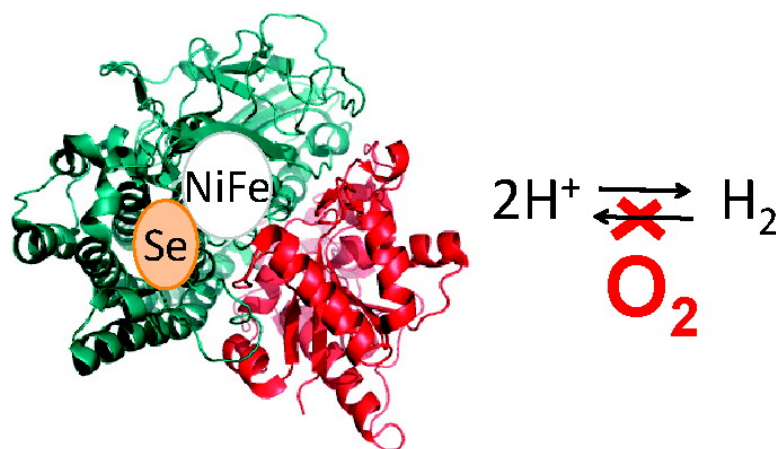
Article

The Difference a Se Makes? Oxygen-Tolerant Hydrogen Production by the [NiFeSe]-Hydrogenase from *Desulfomicrobium baculatum*

Alison Parkin, Gabrielle Goldet, Christine Cavazza, Juan C. Fontecilla-Camps, and Fraser A. Armstrong

J. Am. Chem. Soc., **2008**, 130 (40), 13410-13416 • DOI: 10.1021/ja803657d • Publication Date (Web): 10 September 2008

Downloaded from <http://pubs.acs.org> on February 8, 2009



More About This Article

Additional resources and features associated with this article are available within the HTML version:

- Supporting Information
- Access to high resolution figures
- Links to articles and content related to this article
- Copyright permission to reproduce figures and/or text from this article

[View the Full Text HTML](#)

The Difference a Se Makes? Oxygen-Tolerant Hydrogen Production by the [NiFeSe]-Hydrogenase from *Desulfomicrobium baculatum*

Alison Parkin, Gabrielle Goldet, Christine Cavazza, Juan C. Fontecilla-Camps, and Fraser A. Armstrong*

Inorganic Chemistry, University of Oxford, South Parks Road, OX1 3QR, England, Laboratoire de Cristallogénèse des Protéines, Institut de Biologie Structurale J.-P. Ebel, CEA, CNRS, Université Joseph Fourier, 41, Jules Horowitz, 38027 Grenoble Cedex, France

Received May 16, 2008; E-mail: fraser.armstrong@chem.ox.ac.uk

Abstract: Protein film voltammetry studies of the [NiFeSe]-hydrogenase from *Desulfomicrobium baculatum* show it to be a highly efficient H₂ cycling catalyst. In the presence of 100% H₂, the ratio of H₂ production to H₂ oxidation activity is higher than for any conventional [NiFe]-hydrogenases (lacking a selenocysteine ligand) that have been investigated to date. Although traces of O₂ (\ll 1%) rapidly and completely remove H₂ oxidation activity, the enzyme sustains partial activity for H₂ production even in the presence of 1% O₂ in the atmosphere. That H₂ production should be partly allowed, whereas H₂ oxidation is not, is explained because the inactive product of O₂ attack is reductively reactivated very rapidly, but this requires a potential that is almost as negative as the thermodynamic potential for the 2H⁺/H₂ couple. The study provides further encouragement and clues regarding the feasibility of microbial/enzymatic H₂ production free from restrictions of anaerobicity.

Hydrogenases are microbial metalloenzymes that catalyze the oxidation and production of hydrogen (H₂). The two main classes are known as [NiFe]- or [FeFe]-hydrogenases depending on the metal ion content of their catalytically active site. Crystal structures have been solved for members of both classes: in all cases the active site is buried but linked electrically to the protein surface by an electron relay consisting of at least one Fe–S cluster.¹ At the active site, coordination of iron or iron and nickel by thiolates, CO and CN[−] ligands (Figure 1) results in an extremely efficient catalyst that has been compared, favorably, with platinum, the standard catalyst for H₂ cycling.^{2–4} Despite the chemical similarities in their active sites, the [NiFe]- and [FeFe]-hydrogenases share no amino-acid sequence similarity, and these two solutions to the catalysis of H⁺/H₂ cycling in biology must be the result of convergent evolution.⁵

In view of the importance of H₂ in future energy technologies, it has become crucial to establish the basis by which common first-row transition elements attain such activity by virtue of their coordination shell and supramolecular environment (surrounding protein interior). The technological interest arises not only in developing alternative catalysts for H₂ oxidation (replacing platinum in fuel cells)^{6,7} but also for understanding how organisms could be engineered to give a vastly enhanced

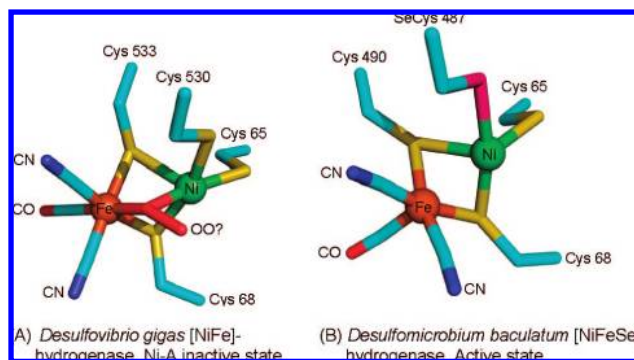


Figure 1. Comparing the structures of [NiFe]- and [NiFeSe]-hydrogenase active sites.¹⁸ The *Desulfovibrio gigas* structure corresponds to an as-prepared oxidized form of a [NiFe]-hydrogenase with a putative bridging (hydro)peroxy ligand with 70% occupancy. This is the Unready or Ni-A form of enzyme.¹⁹ The [NiFeSe]-hydrogenase structure corresponds to a H₂-reduced form of the enzyme and it is in an active state.

H₂ production capability^{8–10} and in developing synthetic catalysts for efficient H₂ production.^{4,11–17}

Hydrogenases can also be classed into those that (predominantly) oxidize H₂ and those that evolve (produce) H₂ through H⁺ reduction; thus, among the various mechanistic issues, it is also important to determine the factors that enable a hydrogenase to function preferentially in one direction versus the other. A particularly interesting substitution that biology has introduced to the [NiFe] active site involves replacement of one of the

* To whom correspondence should be addressed.

- (1) Fontecilla-Camps Juan, C.; Volbeda, A.; Cavazza, C.; Nicolet, Y. *Chem. Rev.* **2007**, *107*, 4273–303.
- (2) Jones, A. K.; Sillery, E.; Albracht, S. P. J.; Armstrong, F. A. *Chem. Commun.* **2002**, 866–867.
- (3) Karyakin, A. A.; Morozov, S. V.; Voronin, O. G.; Zorin, N. A.; Karyakina, E. E.; Fateyev, V. N.; Cosnier, S. *Angew. Chem.* **2007**, *46*, 7244–7246.
- (4) Hambourger, M.; Gervaldo, M.; Svedruzic, D.; King, P. W.; Gust, D.; Ghirardi, M.; Moore, A. L.; Moore, T. A. *J. Am. Chem. Soc.* **2008**, *130*, 2015–2022.
- (5) Vignais, P. M.; Billoud, B. *Chem. Rev.* **2007**, *107*, 4206–4272.

- (6) Vincent, K. A.; Cracknell, J. A.; Clark, J. R.; Ludwig, M.; Lenz, O.; Friedrich, B.; Armstrong, F. A. *Chem. Commun.* **2006**, 5033–5035.
- (7) Vincent, K. A.; Cracknell, J. A.; Lenz, O.; Zebger, I.; Friedrich, B.; Armstrong, F. A. *Proc. Nat. Acad. Sci. U.S.A.* **2005**, *102*, 16951–16954.

terminal cysteine ligands to the nickel by selenocysteine, resulting in the subclass known as [NiFeSe]-hydrogenases. As shown in Figure 1, the active site ligation and geometry of the [NiFeSe] active site is otherwise similar to that of conventional [NiFe]-hydrogenases so far characterized.¹⁸ The bridging ligand present in the [NiFe] active site is due to the fact that the crystal structure has been obtained for an inactive (predominantly Ni-A) form of the enzyme.

In addition to catalyzing H₂/H⁺ cycling, hydrogenases react with O₂, resulting in inactivation due to oxidation and introduction of oxygen-derived species at the active site.²⁰ In general, for [NiFe]-enzymes the inactivation is reversible, and involves oxidation to nickel(III) in conjunction with coordination of a bridging ligand.^{21,22} With conventional [NiFe]-hydrogenases these oxidized inactive states appear to fall into two categories. The so-called Ni-B inactive state, which can also be generated anaerobically, contains nickel(III) with a OH⁻ ligand in the bridging position.²³ The other inactive state is known as Ni-A: it appears that O₂ is essential for its formation but the nature of Ni-A remains controversial with proposals ranging from the presence of a bridging peroxide (HO₂⁻), part A of Figure 1, to one or more cysteine thiolates modified to sulfenates.^{19,24–26} Aside from possessing distinct EPR characteristics, Ni-A and Ni-B are distinguished kinetically because Ni-B is reactivated very rapidly upon reduction under H₂ (hence it is also known as 'Ready'), whereas reactivation of Ni-A is slow and in some cases requires several hours (hence Ni-A is also known as 'Unready').²⁴

This article concerns the properties of the [NiFeSe]-active site in the soluble hydrogenase from *Desulfomicrobium baculatum*,²⁷ which was the subject of the structural investigation

summarized in part B of Figure 1.^{18,28,29} In contrast to the conventional [NiFe]-hydrogenases, for [NiFeSe]-enzymes there is only scant EPR evidence for Ni-A and Ni-B states. Specifically, Teixeira et al. reported³⁰ that aerobically isolated soluble [NiFeSe]-hydrogenase from the periplasm of *D. baculatum* shows only low-intensity EPR signals attributable to Ni-A and/or Ni-B, whereas a sample of the soluble enzyme isolated from the cytoplasm was EPR-silent. These results appear consistent with the observation that the as-isolated (O₂ exposed) enzyme is easily activated, or (most unexpectedly) the active site does not react with O₂.^{30,31} It is not clear how the sequences of periplasmic and cytoplasmic forms of the enzyme differ, if at all. Studies on another [NiFeSe]-hydrogenase, the F420-reducing enzyme from *Methanococcus voltae*, showed³² that oxidation of active enzyme either by O₂ or by dichloroindophenol yielded an EPR spectrum mainly resembling Ni-B in conventional [NiFe]-hydrogenases.

A central issue is how replacement of a single sulfur donor by a selenium donor in such a crucial active site ligand position might alter the properties of the enzyme. There are several differences between sulfur and its heavier group 16 congener selenium, mostly relating to the weaker chemical bonds formed by selenium. A selenol group is more acidic than a thiol (the pK_a of SeCys is 5.2, whereas that of the cysteine thiol is 8.0).³³ This implies that a SeCys could more readily donate a proton to an acceptor in its vicinity, and thus favor H₂ production at the hydrogenase active site. The acidity of SeCys has already been used to justify why in the proton-deuteron exchange reaction the rate of H₂ evolution is higher than that of HD (the H₂/HD ratio is greater than 1.0) for the [NiFeSe]-hydrogenases but not for the [NiFe]-hydrogenases.³⁴ In regard to reactions with O₂ which could modify a cysteine ligand, a Se–O bond should be weaker than a S–O bond, so any oxygen-bound inactive state of the [NiFe] active site should be more easily restored to its normal form in a selenium-containing hydrogenase: this might then provide a protective mechanism and some degree of O₂ tolerance. In the enzymes glutathione peroxidases and *Escherichia coli* formate dehydrogenase H, it is found that Se–O species are essential to activity. The importance of the unique ability for selenium to catalyze this chemistry is demonstrated by the fact that sulfur-containing glutathione peroxidase homologues always prove to be less efficient at reducing lipid hydroperoxides by 2 to 3 orders of magnitude.³³ Similarly in *E. coli* dehydrogenase H, replacement of selenium by sulfur prevents formation of the correct oxygen-species and

- (8) Sakurai, H.; Masukawa, H. *Marine Biotechnol.* **2007**, *9*, 128–145.
 (9) Ghirardi, M. L.; Posewitz, M. C.; Maness, P.-C.; Dubini, A.; Yu, J.; Seibert, M. *Annu. Rev. Plant Biol.* **2007**, *58*, 71–91.
 (10) Basak, N.; Das, D. *World J. Microbiol. Biotechnol.* **2007**, *23*, 31–42.
 (11) Canaguier, S.; Artero, V.; Fontecave, M. *Dalton Trans.* **2008**, 315–325.
 (12) Tye, J. W.; Darensbourg, M. Y.; Hall, M. B. *Inorg. Chem.* **2006**, *45*, 1552–1559.
 (13) Rauchfuss, T. B. *Science* **2007**, *316*, 553–554.
 (14) Schwab, D. E.; Tard, C.; Brecht, E.; Peters, J. W.; Pickett, C. J.; Szilagyi, R. K. *Chem. Commun.* **2006**, 3696–3698.
 (15) Ott, S.; Kritikos, M.; Akermark, B.; Sun, L. C. *Angew. Chem., Int. Edit.* **2003**, *42*, 3285–3288.
 (16) Wilson, A. D.; Shoemaker, R. K.; Miedaner, A.; Muckerman, J. T.; DuBois, D. L.; Dubois, M. R. *Proc. Nat. Acad. Sci. U.S.A.* **2007**, *104*, 6951–6956.
 (17) Hu, X.; Brunschwig, B. S.; Peters, J. C. *J. Am. Chem. Soc.* **2007**, *129*, 8988–8998.
 (18) Garcin, E.; Vernede, X.; Hatchikian, E. C.; Volbeda, A.; Frey, M.; Fontecilla-Camps, J. C. *Structure (London)* **1999**, *7*, 557–566.
 (19) Volbeda, A.; Martin, L.; Cavazza, C.; Matho, M.; Faber, B. W.; Roseboom, W.; Albracht, S. P. J.; Garcin, E.; Rousset, M.; Fontecilla-Camps, J. C. *J. Biol. Inorg. Chem.* **2005**, *10*, 239–249.
 (20) Vincent, K. A.; Parkin, A.; Lenz, O.; Albracht, S. P. J.; Fontecilla-Camps, J. C.; Cammack, R.; Friedrich, B.; Armstrong, F. A. J. *Am. Chem. Soc.* **2005**, *127*, 18179–18189.
 (21) De Lacey, A. L.; Fernandez, V. M.; Rousset, M.; Cammack, R. *Chem. Rev.* **2007**, *107*, 4304–4330.
 (22) Lubitz, W.; Reijerse, E.; van Gestel, M. *Chem. Rev.* **2007**, *107*, 4331–4365.
 (23) Jones, A. K.; Lamle, S. E.; Pershad, H. R.; Vincent, K. A.; Albracht, S. P. J.; Armstrong, F. A. J. *Am. Chem. Soc.* **2003**, *125*, 8505–8514.
 (24) Lamle, S. E.; Albracht, S. P. J.; Armstrong, F. A. J. *Am. Chem. Soc.* **2004**, *126*, 14899–14909.
 (25) Lamle, S. E.; Albracht, S. P. J.; Armstrong, F. A. J. *Am. Chem. Soc.* **2005**, *127*, 6595–6604.
 (26) Gestel, M.; Stein, M.; Brecht, M.; Schroeder, O.; Lenzian, F.; Bittl, R.; Ogata, H.; Higuchi, Y.; Lubitz, W. *J. Biol. Inorg. Chem.* **2006**, *11*, 41–51.

- (27) Hydrogenase was purified from French pressed *Desulfomicrobium baculatum* cells. The final homogeneous enzyme product was assessed by mass spectrometry, with measurement of 55 and 31 kDa for the respective masses of the large and small subunits.
 (28) Menon, N. K.; Peck, H. D., Jr.; Le Gall, J.; Przybyla, A. E. *J. Bacteriol.* **1987**, *169*, 5401–7.
 (29) Teixeira, M.; Moura, I.; Fauque, G.; Dervartanian, D. V.; Legall, J.; Peck, H. D., Jr.; Moura, J. J. G.; Huynh Boi, H. *Eur. J. Biochem.* **1990**, *189*, 381–6.
 (30) Teixeira, M.; Fauque, G.; Moura, I.; Lespinat, P. A.; Berlier, Y.; Prickril, B.; Peck, H. D., Jr.; Xavier, A. V.; Le Gall, J.; Moura, J. J. G. *Eur. J. Biochem.* **1987**, *167*, 47–58.
 (31) Medina, M.; Hatchikian, E. C.; Cammack, R. *Biochim. Biophys. Acta, Bioenergetics* **1996**, *1275*, 227–236.
 (32) Sorgenfrei, O.; Duin, E. C.; Klein, A.; Albracht, S. P. J. *Eur. J. Biochem.* **1997**, *247*, 681–687.
 (33) Birringer, M.; Pilawa, S.; Flohe, L. *Nat. Prod. Rep.* **2002**, *19*, 693–718.
 (34) Vignais, P. M.; Courmac, L.; Hatchikian, E. C.; Elsen, S.; Serebryakova, L.; Zorin, N.; Dimon, B. *Int. J. Hydrogen Energy* **2002**, *27*, 1441–1448.

the hydroxide ligand found in the wild type is replaced by an oxo ligand in the sulfur mutant.³⁵

In this report, the [NiFeSe]-hydrogenase has been probed using protein film voltammetry (PFV). This technique has been previously used to study [NiFe]- and [FeFe]-hydrogenases from the bacteria *Allochromatium vinosum* (*A. vinosum*),^{2,20,23–25,36–40} *Desulfovibrio fructosovorans*,^{41,42} *Desulfovibrio desulfuricans*,^{20,43} *Desulfovibrio gigas* (*D. gigas*),²⁰ *Desulfovibrio vulgaris*,⁴⁰ *Clostridium acetobutylicum*,⁴⁴ *Ralstonia eutropha*,^{7,20} and *Ralstonia metallidurans*.^{5,6} These electrochemical measurements have complemented structural and spectroscopic investigations and added support for assignments of states, for example the proposal that Ni-A and Ni-B differ in oxidation level based on the incorporated oxygen species.²⁴ Strict control over the oxidation states of the hydrogenase is possible because PFV involves adsorbing tiny amounts of redox-active enzyme *directly* onto the surface of an electrode, which ensures direct control over the electrochemical potential sensed by the active sites. Importantly, catalytic activity is recorded directly as an electrical current – positive for oxidation and negative for reduction – and changes in catalytic activity are thus observed as changes in current, as a function of potential and time. High activity translates as a large current and excellent signal-to-noise ratio. Both voltammetry experiments (potential-sweep) and chronoamperometry experiments (the potential is poised at different values) are conducted, and these probe the transformations between active and inactive states.

Methods

The *D. baculatum* hydrogenase sample was obtained and characterized using previously published methods.^{27,45} In conventional assays, the purified enzyme is not fully active but rapidly activates after a few minutes under H₂ to give a specific activity of 1700 μmol H₂ oxidized min⁻¹ (mg hydrogenase)⁻¹. All solutions were prepared with purified water (Millipore 18 MΩ cm) and were pH-buffered using either 0.05 M phosphate or a mixed buffer system. The reagents NaCl, NaH₂PO₄, and Na₂HPO₄ were purchased from Sigma. The phosphate buffer was prepared by mixing NaH₂PO₄ and Na₂HPO₄ to obtain the required pH, and 0.1 M NaCl was present as additional supporting electrolyte. The mixed buffer system consisted of 15 mM in each of sodium acetate, MES (2-(*N*-morpholino)ethanesulfonic acid, Melford), HEPES (*N*'-[2-hydroxyethyl]piperazine-*N*'-2-ethane sulfonic acid, Fisher), TAPS (*N*'-tris[hydroxymethyl]methyl-3-amino propane sulfonic acid, Sigma),

and CHES (2-[*N*'-cyclohexylamino]ethane sulfonic acid, Sigma). The solution was titrated to the desired pH with NaOH and HCl, and 0.1 M NaCl was present as additional supporting electrolyte.

The enzyme film was adsorbed from dilute enzyme solution (containing 0.2 mg mL⁻¹ polymyxin B sulfate as coadsorbate) onto a freshly sanded pyrolytic graphite edge (PGE) electrode (Tufbak Durite sandpaper (Norton) P800) as the potential was cycled once between -558 and +242 mV at 10 mV s⁻¹. This procedure gives a submonolayer film of high electrocatalytic activity. The enzyme can also be adsorbed onto an alumina-polished electrode (1 μm Al₂O₃ from Buehler) and the same characteristic waveshapes (see below) are obtained. Following film growth, the electrode was placed in the electrochemical cell containing 2 mL of pristine mixed buffer. Importantly, no enzyme was present in this solution. For experiments in which we examined nonturnover signals due to the Fe-S clusters (reported in the Supporting Information), we formed the enzyme film on the electrode by spreading a tiny aliquot of concentrated [NiFeSe]-hydrogenase (17 μM enzyme, 14 mM polymyxin B sulfate (Sigma)) on the freshly sanded PGE surface.

All experiments were carried out in an all-glass, thermostatted electrochemical cell equipped for studies under constant gas flow conditions, which was housed in an anaerobic glovebox (M. Braun or Vacuum Atmospheres) with O₂ < 1 ppm. A piece of platinum wire was used as the counter electrode, and the potential was monitored with a saturated calomel reference electrode located in a Luggin sidearm filled with 0.1 M NaCl. The potentials quoted against SHE were obtained by using the correction factor $E_{\text{SHE}} = E_{\text{SCE}} + 0.242\text{V}$ at 25 °C.⁴⁶ The experiments were carried out using PGSTAT 10, PGSTAT 20, or PGSTAT 30 electrochemical analyzers (Eco Chemie) controlled by *GPES* software. Voltammograms were measured in digital-step mode although some experiments (reported in the Supporting Information) were carried out using an analog voltage ramp. Gas composition and flow rate through the cell were manipulated by a set of flow controllers (Smart-Trak series 100, Sierra Instruments). The primary gases from which different mixtures were generated were O₂ (Air Products), CO (Research grade, BOC), 1% CO in N₂ (BOC), and N₂ (Oxygen-free, BOC). In the experiments where gases were injected as saturated solutions, the concentration in the cell was estimated using standard Henry's Law constants, from the saturated concentration of gas and the dilution factor involved.

Results

1. Oxidation and Production of H₂ under Anaerobic Conditions. We first performed experiments to ascertain the general characteristics of electrocatalysis by *D. baculatum* [NiFeSe]-hydrogenase operating in either H₂ oxidation or H⁺ reduction directions. In Figure 2, we show cyclic voltammograms measured under various conditions designed to obtain a general picture of the catalytic properties as a function of electrode potential. Greater stability was obtained when a lower temperature (25 °C) was used, but to observe more clearly the anaerobic inactivation, a higher temperature (45 °C) was required. The voltammograms (scan rate 10 mV s⁻¹) in part A of Figure 2 were measured for the same film of enzyme at 25 °C, pH 6.0, changing the gas in the headspace between first 100% H₂, then 100% argon and finally 5% H₂ in N₂. Five minutes were allowed between each cycle to allow for equilibration before commencing the next scan.

Under 100% H₂, 25 °C (part A of Figure 2), an unusual, almost linear current response is observed. We have previously observed similar results for other enzymes and suggested that the linear response is due to enzyme molecules being adsorbed in a variety of different configurations relative to the rough and

(35) Axley, M. J.; Boeck, A.; Stadtman, T. C. *Proc. Nat. Acad. Sci. U.S.A.* **1991**, *88*, 8450–4.

(36) Pershad, H. R.; Duff, J. L. C.; Heering, H. A.; Duin, E. C.; Albracht, S. P. J.; Armstrong, F. A. *Biochemistry* **1999**, *38*, 8992–8999.

(37) Léger, C.; Jones, A. K.; Albracht, S. P. J.; Armstrong, F. A. *J. Phys. Chem. B* **2002**, *106*, 13058–13063.

(38) Léger, C.; Jones, A. K.; Roseboom, W.; Albracht, S. P. J.; Armstrong, F. A. *Biochemistry* **2002**, *41*, 15736–15746.

(39) Lamle, S. E.; Vincent, K. A.; Halliwell, L. M.; Albracht, S. P. J.; Armstrong, F. A. *Dalton Trans.* **2003**, 4152–4157.

(40) Vincent, K. A.; Belsey, N. A.; Lubitz, W.; Armstrong, F. A. *J. Am. Chem. Soc.* **2006**, *128*, 7448–7449.

(41) Léger, C.; Dementin, S.; Bertrand, P.; Rousset, M.; Guigliarelli, B. *J. Am. Chem. Soc.* **2004**, *126*, 12162–12172.

(42) Dementin, S.; Belle, V.; Bertrand, P.; Guigliarelli, B.; Adryanczyk-Perrier, G.; De Lacey, A. L.; Fernandez, V. M.; Rousset, M.; Léger, C. *J. Am. Chem. Soc.* **2006**, *128*, 5209–5218.

(43) Parkin, A.; Cavazza, C.; Fontecilla-Camps, J. C.; Armstrong, F. A. *J. Am. Chem. Soc.* **2006**, *128*, 16808–16815.

(44) Baffert, C.; Demuez, M.; Cournac, L.; Burlat, B.; Guigliarelli, B.; Bertrand, P.; Girbal, L.; Léger, C. *Angew. Chem.* **2008**, *47*, 2052–2054.

(45) Hatchikian, E. C.; Bruschi, M.; Le Gall, J.; Forget, N.; Bovier-Lapierre, G. *Biochem. Biophys. Res. Commun.* **1978**, *82*, 451–61.

(46) Bard, A. J.; Faulkner, L. R. *Electrochemical Methods: Fundamentals and Applications*, 1980.

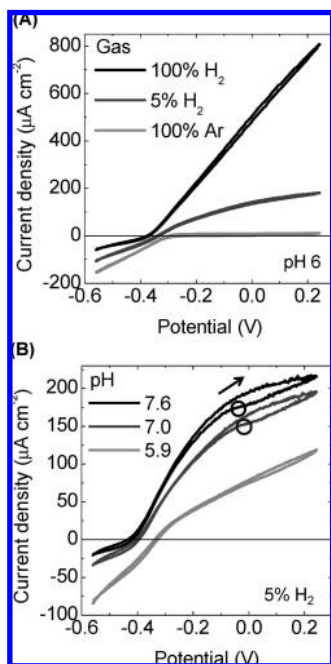


Figure 2. How the bidirectional activity of *Desulfomicrobium baculatum* [NiFeSe]-hydrogenase varies with (A) gas atmosphere and (B) pH. 10 mVs^{-1} scans measured (A) under different gas atmospheres (1 bar pressure) as shown in the legend and (B) at different pH under an atmosphere of 5% H_2 , 95% N_2 . (A) Between each gas exchange, 5 min was allowed for equilibration with the solution, the gases were interchanged between 100% H_2 , 100% argon, and 5% H_2 . (B) The pH of the electrochemical cell solution was lowered by stepwise solution exchanges from 7.6 to 7.0 to 5.9 with 5 min equilibration pauses between each experiment. The pH was rechecked immediately after each experiment. The arrow on the pH 7.6 scan emphasizes the scan direction of the line immediately below it and circles on the pH 7.6 and pH 7.0 scans denote inflection points on the return scan, attributable to reactivation of small amounts of an oxidized inactive state. Other conditions: electrode rotation 3000 rpm, mixed buffer, 25 °C for scans in (A) and 45 °C for scans in (B), gas exchange and pH exchange data were obtained on separate enzyme films.

irregular graphite surface, so that there is a dispersion of electron-transfer distances and interfacial electron-transfer rate constants.³⁷ The linearity is related to the catalytic activity of the enzyme and the ratio between its turnover frequency and the standard interfacial rate constant.³⁷ The voltammetry, in concurrence with the measured specific activity (which is comparable to that of *D. gigas* [NiFe]-hydrogenase), shows that [NiFeSe]-hydrogenase is a very active enzyme for H_2 oxidation, even though the electrode kinetics are far from ideal for many of the molecules involved. Under 5% H_2 , the current response due to H_2 oxidation is curved, reflecting some oxidative inactivation, as discussed below. As the H_2 level in the headgas is increased from 0 to 5 to 100%, the H^+ reduction current decreases but it is still very evident at 100% H_2 (1 bar).

In part B of Figure 2, we show voltammograms measured at 45 °C, under 5% H_2 in N_2 , for different pH values. The traces cut across the zero-current axis at potentials coinciding with the reduction potential of the $2\text{H}^+/\text{H}_2$ couple under the same conditions (-438 mV pH 7.6, -401 mV pH 7.0, -331 mV pH 5.9). This steep intersection across the zero-current axis demonstrates that both H_2 oxidation and H^+ reduction occur with minimal overpotential. At pH 7.6 and 7.0, the H_2 oxidation activity levels off at high potential. This is attributed to anaerobic inactivation, and such behavior has been observed for all hydrogenases studied to date.⁴⁷ Reductive reactivation of the small number of enzyme molecules that have become inactive

during the cycle is identified by a discernible inflection point at which current loss occurs less rapidly between 0 and -0.1 V (pH dependent), as circled in the return scan. The fact that these processes are not detected at a higher H_2 concentration suggests that H_2 binding protects the enzyme from high-potential anaerobic inactivation, and this proposal is currently under detailed investigation. Potential-step chronoamperometry experiments examining the effect of electrode potential (driving force) on the rate of the inactivation and reactivation processes revealed (Supporting Information) that the rate of inactivation is independent of potential ($61 \rightarrow 241$ mV) and the rate of reactivation increases over the range $61 \rightarrow 1$ mV.

If the electroactive coverage of enzyme is known, the turnover rate of the enzyme at any potential and substrate can be determined.⁴⁸ Our attempts to determine the electroactive coverage of the hydrogenase produced only a weak peak-like response at 1 °C under the conditions of an analog voltage ramp that is necessary for absolute integration to obtain the charge passed (Supporting Information). From voltammograms executed in digital-step mode (also shown in the Supporting Information), which for an immobilized redox species produces an amplification,⁴⁹ we observed a single signal, consisting of peaks in oxidation and reduction directions, consistent with all electron-transfer centers having similar reduction potentials. From the tiny size of the voltammetric signal obtained in analog mode, we concluded that the electroactive coverage in typical experiments must be less than 1×10^{-12} moles cm^{-2} . Thus, a current density of 0.8 mA cm^{-2} at 0.24 V under 100% H_2 corresponds to a turnover frequency of at least 4000 s^{-1} (molecules H_2 oxidized). For H^+ reduction under 100% argon, the current density of 0.15 mA cm^{-2} at -0.55 V led, similarly, to an estimate of at least 750 s^{-1} (molecules H_2 produced). The [NiFeSe]-hydrogenase is therefore also a good H_2 producer.

2. Effect of O_2 on H_2 Oxidation. The [NiFeSe]-hydrogenase does not support H_2 oxidation activity in the presence of O_2 . As shown of Figure 3A, during cyclic voltammetry, injecting 0.2 mL of O_2 -saturated buffer into 2 mL of cell solution (resulting in 9% O_2 i.e. approximately 118 μM at 30 °C) immediately abolishes the current due to oxidation of (originally) 100% H_2 . The scan rate is so slow (1 mV s^{-1}) that the O_2 has been removed from the solution by the time the cycle is reversed, and features (circled) due to reactivation processes are observed. In a further experiment (part B of Figure 3) also with 100% H_2 but carried out at constant potential (0.24 V vs SHE), O_2 was injected to give a final concentration of 0.5% (7 μM), and complete and rapid inactivation was again observed ($>50\%$ is lost in the first 2 s). As found for other [NiFe]-hydrogenases, the O_2 -inactivation is essentially reversible upon reduction. Unusually, the reactivation current–potential profile measured for the sweep to more negative potential (shown in detail in part C of Figure 3) reveals two different species that are distinguished because they reactivate at completely different potentials. The catalytic current decreases between the first and second activation process because as the potential becomes more negative there is a smaller thermodynamic driving force for H_2 oxidation. It is important to note that part C of Figure 3 does not convey the true relative quantities of the two species. In particular, activation of the low-potential species occurs close to the potential

(47) Vincent, K. A.; Parkin, A.; Armstrong, F. A. *Chem. Rev.* **2007**, *107*, 4366–4413.

(48) Hudson, J. M.; Heffron, K.; Kotlyar, V.; Sher, Y.; Maklashina, E.; Cecchini, G.; Armstrong, F. A. *J. Am. Chem. Soc.* **2005**, *127*, 6977–6989.

(49) Heering, H. A.; Mondal, M. S.; Armstrong, F. A. *Anal. Chem.* **1999**, *71*, 174–182.

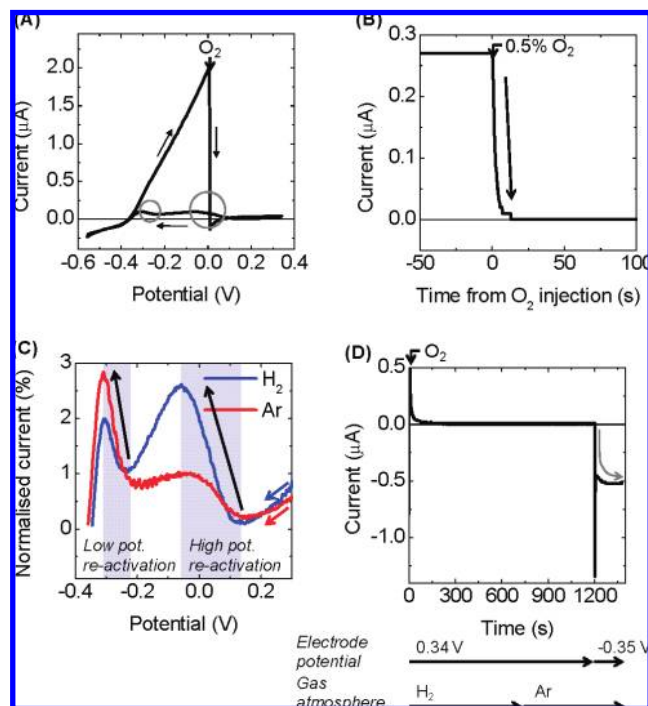


Figure 3. Reaction of *Desulfomicrobium baculatum* [NiFeSe]-hydrogenase with O_2 . (A) Cyclic voltammogram recorded at 1 mVs^{-1} , starting from -558 mV then scanning to $+342 \text{ mV}$ and returning, under 100% (1 bar) H_2 . At 0 mV on the positive direction scan, O_2 -saturated buffer was injected (indicated by the vertical arrow) and then rapidly removed by flushing the headspace in the electrochemical cell with H_2 . (B) Current–time trace for inactivation at 0 V by $0.5\% O_2$ in $5\% H_2$ ($95\% N_2$). (C) Reactivation following injection of O_2 at high potential under an argon or H_2 atmosphere. Prior to both scans, the electrode potential was swept from -558 to $+342 \text{ mV}$ and the maximum H_2 oxidation current was noted. The electrode was then polarized at -558 mV under $100\% H_2$ to ensure complete activation of the enzyme film. For the argon experiment, the gas space in the electrochemical cell was then flushed with argon for 5 min to remove H_2 . Immediately after a potential step to $+342 \text{ mV}$, $200 \mu\text{L}$ of O_2 -saturated buffer was injected into the 2 mL cell solution, and the headspace was flushed to remove O_2 with argon for 300 s then with H_2 for 300 s . The electrode potential was then scanned to more negative potentials at 1 mVs^{-1} , as shown, with current normalized with respect to the maximum activity that was first measured at $+342 \text{ mV}$ under $100\% H_2$. For the H_2 experiment, the same maximal activity measurement, potential step, injection method, and scanning measurement were employed but no argon was used. (D) An experiment to determine the rate of reactivation of *D. baculatum* [NiFeSe]-hydrogenase H_2 production activity following O_2 inactivation at high potential. The electrode potential was poised at -550 mV for 500 s to fully activate the enzyme under $100\% H_2$ (not shown). The potential was then stepped to $+340 \text{ mV}$ and $150 \mu\text{L}$ of O_2 -saturated buffer was immediately injected to inactivate the enzyme. For the next 1200 s , the electrode potential was maintained at $+340 \text{ mV}$ to ensure all O_2 was flushed from the cell, and the headgas was changed from H_2 to argon. The electrode potential was then stepped down to -350 mV to induce activation of H_2 production catalysis. Conditions: pH 6, electrode rotation rate at least 2500 rpm , $30 \text{ }^\circ\text{C}$, 1 bar H_2 or argon, (A) and (C) mixed buffer, (B) and (D) phosphate buffer.

at which H_2 oxidation activity ceases and is replaced by H^+ reduction. (Note that the percentage current is arbitrarily normalized with respect to the H_2 oxidation current measured at $+342 \text{ mV}$ prior to O_2 being added.) The relative proportions of the high-potential and low-potential reactivating species could be altered by changing the gas atmosphere under which O_2 injection took place. The process at high potential, enhanced by injecting O_2 under H_2 (rather than argon), is indistinguishable in terms of potential from that occurring after anaerobic inactivation, whereas the low-potential process, enhanced by injection of O_2 under argon, appears

quite close to the formal potential for the H^+/H_2 couple (ca. -350 mV at pH 6) and is not detected after anaerobic inactivation.

Observation of the low-potential (O_2 -specific) reactivation process led us to question how fast this species could be reactivated by reduction. Because the window remaining within the H_2 oxidation region is so narrow, it was necessary to employ potential steps into the H^+ reduction region. A result is shown in part D of Figure 3 where O_2 was injected during H_2 oxidation (1 bar) at a potential of 0.34 V . This resulted in rapid and complete inactivation. After 5 min , the headgas was changed to 100% argon; then 5 min later the potential was stepped to -0.35 V , a potential at which H^+ reduction will occur under these conditions (part A of Figure 2). Most of the enzyme was reactivated within the current spike (i.e., within seconds).⁵⁰ This was confirmed in numerous other experiments: using a more negative reactivation potential (below -0.38 V) all the reaction occurred within the spike. Reactivation after treatment with O_2 is therefore fast in this potential region.

3. H_2 production in $1\% O_2$. Because reactivation of the O_2 -specific inactive species only occurs rapidly at electrode potentials close to the thermodynamic potential of the H^+/H_2 couple, there is no possibility that this [NiFeSe]-hydrogenase could oxidize H_2 in the presence of O_2 . However, the reactivation reaction is fast, and this suggested that it might be possible, instead, to achieve sustainable H_2 production in the presence of small quantities of O_2 . We therefore designed an experiment to establish and quantify this possibility. It is important to note that inherently rapid reactivation after O_2 attack is also a characteristic of membrane-bound hydrogenases from *Ralstonia* species, and because the process in these enzymes occurs at a high potential it allows H_2 oxidation to proceed in air.^{6,7,20} However, unlike the [NiFeSe] enzyme, the *Ralstonia* hydrogenases are very poor at producing H_2 .

A bare PGE electrode begins to reduce O_2 at potentials more negative than approximately 0 mV at pH 6 (Supporting Information); therefore reduction (negative) current alone could not be used to measure H_2 production activity in O_2 . Instead, the competitive inhibitor CO was used to remove the component in the reduction current arising from enzymatic catalysis. In the Supporting Information, we show voltammograms for O_2 and H_2O_2 reduction at bare PGE and discuss the correction procedure adopted to estimate the amount of O_2 remaining in the diffusion layer to be seen by the [NiFeSe] active site. For our experiments, at an electrode potential of -0.45 V , $1\% O_2$ in the headspace equates to at least $0.5\% O_2$ at the electrode surface.

The experiments shown in Figure 4 measure the H^+ reduction activity when the headgas contains $1\% O_2$ – easily sufficient to abolish all H_2 oxidation activity. In (A), the experiment begins with the PGE electrode modified with a fresh film of [NiFeSe]-hydrogenase being exposed to 1 bar (100%) N_2 while rotating at 3000 rpm at -450 mV . This experiment was carried out at $30 \text{ }^\circ\text{C}$, and the loss of current during the first 500 s is due to a substantial rate of film loss⁵¹ at this temperature. After about 600 s , $1\% CO$ is introduced into the cell through the flowing gas stream. There was an immediate attenuation ($80\text{--}90\%$) of the H^+ reduction current. Then, after a further 200 s , the gas stream was switched back to $100\% N_2$, resulting in an immediate increase in reduction (negative) current to a value about 80% of that recorded before introducing CO (reflecting the film loss

(50) Hirst, J.; Armstrong, F. A. *Anal. Chem.* **1998**, *70*, 5062–5071.

(51) The term *film loss* refers to the steady decrease in current attributed to the processes of: enzyme desorption, enzyme denaturation, and unfavorable conformational rearrangement on the electrode surface.

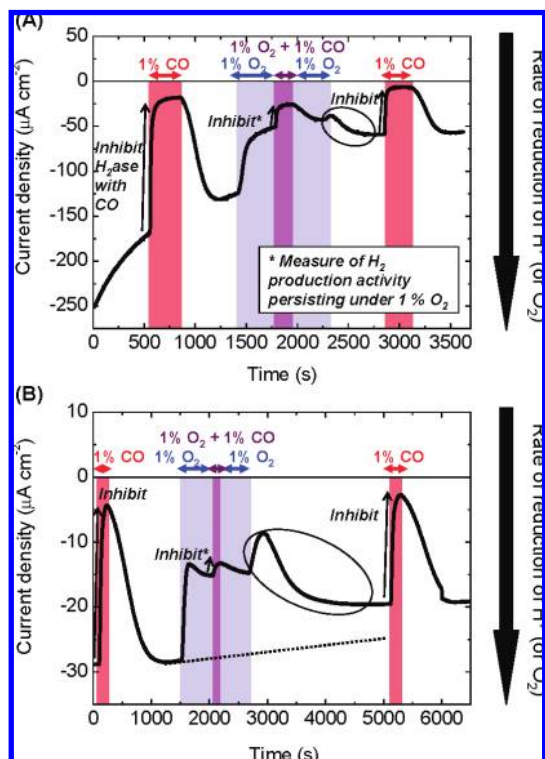


Figure 4. Probing the capacity for O₂ tolerance during H₂ production by *Desulfomicrobium baculatum* [NiFeSe]-hydrogenase. The enzyme was poised at low potential (−0.45V vs SHE) under changing atmospheres of N₂, 1% CO in N₂, 1% O₂ in N₂, and 1% O₂ + 1% CO in N₂ as indicated on the plot. Other conditions: pH 6.0, electrode rotation rate 3000 rpm, phosphate buffer (A): 30 °C and (B): 20 °C. The features circled in (A) and (B) result from flushing O₂ out of the cell and are explained in detail in the main text. The dashed line in (B) delineates an estimate of the course of film loss throughout the experiment. In (B) at 6000 s, the data recording ended and had to be restarted. The apparent small, vertical increase in reduction current at this time results from this loss of data.

over the 800 s of CO inhibition). In the next stage, the gas flow was changed to 1% O₂ in N₂, and this produced a decrease in reduction current that was largely complete after 600 s; at this point the gas flow was switched to 1% O₂, 1% CO, and 98% N₂, resulting in an immediate attenuation. The magnitude of the attenuation (marked by Inhibit* in Figure 4) corresponds to the level of enzymatic H⁺ reduction (H₂ production) persisting when 1% O₂ is in the headgas, and we note that at this stage, about 50% of the current is due to enzyme-catalyzed H⁺ reduction. When CO was removed with a stream of 1% O₂ and 99% N₂, the current increased to a level similar to that recorded prior to CO inhibition. In the third stage of the experiment, the atmosphere was changed to 100% N₂. This resulted in the feature circled in (A): initially there was a small decrease in reduction current (due to loss of O₂ reduction), which was followed by a larger increase in current to reach a steady level as the last traces of O₂ are removed from solution. The gas stream was then switched to 1% CO/99% N₂ to record the amount of active enzyme remaining on the electrode and finally back to 100% N₂ to confirm reversibility. Control experiments showed that no current changes were observed for a bare PGE electrode when CO was either added or removed from a 1% O₂ gas stream (Supporting Information).

The same method was employed in (B). Because a lower temperature (20 °C) was applied, gas equilibration times were slower, and the experiment was therefore conducted over a longer time scale. At this cooler temperature, the rate of film

loss was decreased so the data are less convoluted by a steady loss of enzyme activity over time. Upon introduction of O₂ at 1500 s, the reduction current decreases immediately, reaching a minimum at 1600 s. This is due to rapid inhibition of hydrogenase-catalyzed H₂ production. The reduction current then slowly increases to a stable level of −15 µA cm^{−2} because the current due to O₂ reduction increases as O₂ equilibrates with the solution. This feature was absent in (A) because the magnitude of H₂ production current is much larger than that of O₂ reduction; O₂ inhibition of H₂ production is therefore the predominant characteristic in this phase of the experiment (A). The feature circled in (A) (loss of reduction current upon immediate removal of O₂, followed by an increase in reduction current due to release of O₂ inhibition of the enzyme) is accentuated in (B). This reflects the greater enzyme activity observed in (A) due to temperature and possibly, variation in enzyme coverage. Part B of Figure 4 also shows a projected line indicating the path of film loss. The discrepancy between projected and actual current suggests that some less reversible changes are occurring.

At 30 °C (part A of Figure 4), the fraction of activity persisting when the enzyme is experiencing at least 0.5% O₂ (1% in the headspace: Supporting Information) lies between 17% (based on activity immediately prior to first introduction of CO) and 42% (based on activity immediately prior to final introduction of CO). At 20 °C (part B of Figure 4), the corresponding limits are 7–10%. The O₂ tolerance of the [NiFeSe]-hydrogenase is apparently greater at higher temperature.

Discussion

Our results demonstrate that the [NiFeSe]-hydrogenase from *D. baculatum* is a good H₂ producer; this is true even in the presence of a substantial level of H₂, which is usually a strong inhibitor of H₂ production by [NiFe]-hydrogenases. Our work also shows, clearly, that O₂ reacts with the enzyme, reversibly, causing inactivation, although we cannot comment on the level to which more substantial long-term damage occurs to the enzyme. As shown in Figure 3, reaction of the enzyme with O₂ produces two different inactive species that are clearly distinguished by the potentials at which they undergo rapid reactivation. The minority species, activated at high-potential, is also formed upon anaerobic inactivation, and it reactivates rapidly (half-life of a few seconds) at potentials more negative than 0 V at pH 6. The low-potential species is only formed upon reaction with O₂ under which condition it is the dominant product, and it is reactivated rapidly (a few seconds) but only when the electrode potential is taken below −0.3 V (pH 6). Figure 4 shows further that the apparent rate of reactivation depends critically on removal of the last traces of O₂ (compare the slow increase in activity at −0.45 V as O₂ is expelled, with rapid increase being observed (part D of Figure 3) when reactivation is initiated by a potential step in the absence of O₂).

Rates of reactivation for both of the inactive [NiFeSe] species are much higher than measured for the unready (Ni–A) form of *A. vinosum* [NiFe]-hydrogenase for which the limiting (maximum) rate constant is 0.0025 s^{−1}, corresponding to a half-life of 280 s at 45 °C.²⁴ There is, therefore, a rate increase of about 10² fold for reactivating the O₂-inactivated [NiFeSe]-hydrogenase. The catch is that rapid reactivation requires such a negative potential that it prohibits any H₂ oxidation activity in the presence of O₂; consequently, the [NiFeSe]-hydrogenase cannot be an O₂-tolerant hydrogenase in the direction of H₂ oxidation. In this respect, the enzyme resembles the [NiFe] analogues from *A. vinosum*, *D. vulgaris*, *D. gigas*, and *D. fructosovorans* but not the O₂-tolerant

[NiFe]-hydrogenases from *Ralstonia*, which reactivate rapidly at much higher potentials.^{20,41} It is also interesting that the presence of an H₂ atmosphere is not a requirement to complete the reactivation of the [NiFeSe]-hydrogenase at very negative potentials.²⁵ This may also be true for other hydrogenases when subjected to sufficiently low potentials.

The ability to sustain H₂ production in the presence of 100% H₂ and the activity-potential profile of recovery from O₂ exposure together make the [NiFeSe]-hydrogenase uniquely identifiable from selenium-free counterparts so far investigated. The O₂-sensitivity of hydrogenases has been described as a major limitation to the development of technologies harnessing solar powered bio-H₂ production.^{8,9} Most obviously, hydrogenases operating in photosynthesizing oxygenic organisms must be able to do so in the presence of O₂, the actual amounts depending on light intensity and other conditions. It is widely acknowledged that [NiFe]-hydrogenases are superior in surviving exposure to O₂ when compared to [FeFe]-hydrogenases.⁹ In this light therefore, it has been suggested that cyanobacteria (which produce [NiFe]-hydrogenases rather than [FeFe]-hydrogenases) offer a better practical solution.^{8,9,52,53} Our study now demonstrates the importance of the kinetics and thermodynamics of reactivation after O₂ attack and suggests that, by this principle, it could be possible for a [NiFeSe]-hydrogenase to sustain useful levels of H₂ production activity in low-O₂ atmospheres.

On the basis of the parallels with conventional [NiFe]-hydrogenases, we propose that the inactive species that reactivates at a very low-potential is functionally equivalent to a Ni-A state because it is formed only upon reaction with O₂, and more of this species is formed if O₂ is introduced when H₂ is absent.²⁴ A seemingly contradictory observation is that this species is reactivated rapidly, whereas Ni-A in enzymes such as *A. vinosum* [NiFe] hydrogenase is associated with *slow* reactivation, hence the term Unready;^{20,54} however, at any potential higher than -0.2 V, this state of the [NiFeSe] enzyme is reactivated only very slowly. The observation of a clear *electrochemical* distinction (i.e., in reduction potential) between the inactive product formed anaerobically and that formed only upon reaction with O₂, is so far specific to the [NiFeSe]-hydrogenase.²⁰ Two further aspects deserve to be noted. First, the low-potential inactive species should be stable above -0.2 V and readily available for spectroscopic examination; yet studies of the *D. baculatum* [NiFeSe]-hydrogenases have not revealed any major signals attributable to nickel(III) states formed upon exposure to O₂.³⁰ Second, the study by Sorgenfrei et al. of the F420-reducing [NiFeSe]-hydrogenase from *M. voltae*³² showed that reaction with O₂ produced a species resembling Ni-B not Ni-A.⁵⁵ The electrochemically observed anaerobic inactivation in this study also suggests formation of a Ni-B-like state by a

[NiFeSe]-hydrogenase, and in agreement with previous *A. vinosum* [NiFe]-hydrogenase studies,²³ formation of this state proceeds via a chemical-electrochemical (CE) reaction (a chemical process such as ligand binding followed by a one-electron oxidation of the NiFe site). Subsequent reactivation of this species occurs at high potential via an EC mechanism. It is surprising that oxidized inactive states of the [NiFeSe]-hydrogenases have been difficult to track down by EPR, yet two forms are easily distinguished electrochemically.

Finally, we ask: What unique structural features contribute to the unusual reactivities of the [NiFeSe]-hydrogenase? The two fundamental differences between the architecture of the [NiFeSe]-hydrogenase and typical [NiFe]-hydrogenases from sulfate reducing bacteria are (1) the presence of a selenium atom at the active site, and (2) the absence of a [3Fe-4S]-cluster, which normally has a much higher potential. The lower p*K*_a of RSeH compared to RSH may account for higher H₂ production activities as proposed above.³⁴ Another interesting question is whether the inactive states contain Se-O products analogous to oxygenated sulfur species that may be formed in the [NiFe]-hydrogenases.⁵⁶ However, a Se-O species ought to be reduced at a higher potential than a S-O species, whereas we observe that reductive reactivation requires an unusually negative potential. Importantly though, the reactivation that occurs at this low potential is (thus far) unusually rapid for an O₂-inactivated hydrogenase. With regard to the effect of an absence of a [3Fe-4S] cluster, we note that other hydrogenases having a relatively high bias for H₂ production include the [FeFe]-hydrogenases from *D. desulfuricans* and *C. acetobutylicum*, neither of which contains a [3Fe-4S] cluster.^{4,43}

Whatever the atomic nature of the inactive states, this research has helped to emphasize the importance of the kinetics and thermodynamics of reactivation in the complex and no-doubt multiple mechanisms of O₂ tolerance of hydrogenases, and the results prompt more detailed crystallographic and spectroscopic studies of the [NiFeSe]-enzymes.

Acknowledgment. The research of G. Goldet, A. Parkin, and F. A. Armstrong was supported by grants from BBSRC (BB/D52222X) and EPSRC. C. Cavazza and J. C. Fontecilla-Camps acknowledge the CEA, CNRS and ANR (DIVHYDO) for institutional funding. We thank Sophie Lamle and Kylie Vincent for initial experiments and helpful comments. A. Parkin is grateful to Jesus College, Oxford, for support throughout her graduate studies. The authors gratefully acknowledge Marielle Bauzan for growing the bacteria (Fermentation unit, CNRS, Marseilles, France).

Supporting Information Available: This material is available free of charge via the Internet at <http://pubs.acs.org>.

JA803657D

- (52) Cournac, L.; Guedeney, G.; Peltier, G.; Vignais, P. M. *J. Bacteriol.* **2004**, *186*, 1737–1746.
(53) Dawar, S.; Masukawa, H.; Mohanty, P.; Sakurai, H. *Proc. Indian Natl. Sci. Acad.* **2006**, *72*, 213–223.
(54) Armstrong, F. A.; Albracht, S. P. J. *Philos. Trans. R. Soc. London, Ser. A* **2005**, *363*, 937–954.

- (55) However, in Figure 4 of that article another minority species is observable, which could be attributable to Ni-A.
(56) Fontecilla-Camps, J., C.; Volbeda, A.; Cavazza, C.; Nicolet, Y. *Chem. Rev.* **2007**, *107*, 4273–303.